JEE Journal of Ecological Engineering

*Journal of Ecological Engineering*, 2025, 26(3), 135–146
https://doi.org/10.12911/22998993/199588
ISSN 2299–8993, License CC-BY 4.0

Received: 2025.12.05
Accepted: 2025.01.15
Published: 2025.02.01

# Environmentally friendly synthesis of silver oxide nanoparticles using leaf extract from trumpet vine

Vian I. Mohamad[1], Abeer I. Alwared[1*]

[1] Department of Environmental Engineering, College of Engineering, University of Baghdad, Iraq
* Corresponding author's e-mail: dr.abeer.wared@coeng.uobaghdad.edu.iq

## ABSTRACT

Azo dyes represent a significant concern to the environmental regulations and proper wastewater treatment is crucial in mitigating its impact on ecosystems. This study investigates the removal of black azo dye from aqueous solution using silver oxide nanoparticles ($Ag_2O$ NPs) improved with green-like material. The trumpet vine leaf extracted was used as a capping and reducing agent to formulate the nanomaterial catalyst. A characteristics analysis using scanning electron microscopy (SEM), Energy-Dispersive X-ray Spectroscopy (EDS), X-ray diffraction (XRD), Brunauer-Emmett-Teller (BET), Barrett-Joyner-Halenda (BJH), and Fourier-Transform Infrared Spectroscopy (FTIR) techniques was performed to examine the features of the catalyst. About 79% removal efficiency of azo black dye was reached using a 1.0 g/L dosage of the $Ag_2O$ nanoparticles under visible light exposure in batch mode reactor. The reusability analysis illustrates a stable behavior after five cycles of loading, and the kinetic study revealed that the reaction is compatible with the 1st order kinetic model. These findings suggest an effective, reliable, and bio-friendly photocatalytic candidate for a variety of water treatment applications.

**Keywords:** black azo dye, silver oxide nanoparticle, bio-synthesis, nanomaterial characterization, photocatalysis.

## INTRODUCTION

Water resources are required for the survival of all living beings on earth; thus, water is a vital element for the life in ecosystem. Industrialization inevitably declines quality of sea water and quantity of drinkable water, ultimately endangering marine and human life (Rasouli et al., 2024). Different sources of pollutants such as dyes. About 20% of all dye pollution is reportedly released into the water's surface (Donkadokula et al., 2020). The textile industry has been shown to be a particularly high source of pollutants, generating a significant amount of wastewater daily. Its affluent often contains a high concentration of organic compounds, dyes, and other nutrients, which, if not treated properly, can lead to major environmental pollution, such as acarbose, and rhodamine-610. Even at concentrations less than 1 mg/L, the presence of traces of dye in water is very apparent and influences the aesthetic value of lakes, rivers, and other water bodies, impacting their water transparency and gas solubility. However, dyes are more difficult to handle than other contaminants because of their artificial origin and complex aromatic structures (Alwared et al., 2023a). Azo dyes are the main type of dyes used in the industry, they are the major dyeing process components utilized in the textile industry (Sarkar et al., 2020). They are part of the biggest textile dye family, which includes 60–70% of all textile colors used in practical applications (Sinha et al., 2018). The environment and the general public's health are seriously threatened by these hazardous substances. (Singh et al., 2015). The effective removal of dyes from wastewater is one of the major environmental challenges in water management. To date, various methods of wastewater treatment such as adsorption, electrochemistry, biological treatment, chemical oxidation, coagulation, flocculation, and ion exchange, have been used (Raghad and Abeer, 2023). However, many of these methods have significant drawbacks, such as high costs, the need for complex conditions for the reaction, or the fact that they do little more than transform the contaminants from

liquids to solids, as is the case with most adsorption techniques (Ledakowicz and Paździor, 2021). Advanced oxidation processes (AOPs) are an efficient destructive technique that breaks down organic pollutants into simple products. These processes depend on in-situ generation of •OH radicals to initiate the oxidation reactions, leading to complete mineralization of pollutants to $H_2O$ and $CO_2$. Among these AOPS methods, photocatalysis is considered a relatively attractive option for wastewater treatment and dye decomposition. The photocatalytic process is characterized by low cost, simplicity, high efficiency, and harvesting the solar light to degrade organic pollutants using solid photocatalysts (Okab, and Alwared, 2023).

Silver is one of the less expensive noble metals (Au, Pd). Because of its large surface area, non-toxicity, cost-effectiveness, and environmental friendliness, silver nanoparticles (NPs) are drawing interest in nanotechnology (Aravind et al., 2021). $Ag_2O$, among other semiconductors, demonstrates the best photocatalytic performance when it comes to treating azo dyes because of its rapid rate of photodegradation when exposed to visible light (Wang et al., 2020). $Ag_2O$ is a p-type semiconductor with a brown color and a straightforward cubic structure (Yong and Schoonen, 2000). Its band-gap energy of 1.2 eV is almost perfect, making it appropriate for photocatalytic uses in the visible spectrum. $Ag_2O$ is also widely utilized in a variety of industrial applications, such as electrode materials, cleaning agents, preservatives, colorants, and photocatalysts for organic transformation and environmental remediation. $Ag_2O$ is also discovered to be a stable and extremely effective photocatalyst under visible light (Kadam et al., 2016)

The chemical synthesis for the nanoparticle process involves the chemical reaction of several precursors to produce another nanometer-sized material. The drawbacks of physical and chemical methods are the use of toxic solvents, hazardous waste, and high energy consumption (Narayanan and Sakthivel, 2010). As a result, further developments are required to create ecologically safe and renewable nanoparticles.

The biosynthetic process (also known as green synthesis) is a technique for creating nanoparticles that utilize reducing agents obtained from plants and microorganisms. It offers several advantages, including environmental safety, economic effectiveness, biocompatibility, renewable energy, and non-toxicity. Jalill et al. (2016). Sugars, terpenoids, polyphenols, alkaloids, phenolic acids, and proteins are all compounds that can play a role in the biosynthesis of nanoparticles (Akhtar et al., 2013; Hemlata et al., 2020; Parveene et al., 2016).

Plant-assisted reduction, which is the outcome of phytochemicals such carboxylic acids, amides, aldehydes, and ketones, is the mechanism employed in this process. It is a bottom-up method wherein an oxidation or reduction reaction takes place to create silver nanoparticles (Manik et al., 2020). The green biosynthetic method's basic foundation was bioremediation, a technique that uses plants' natural processes to recover metals from previously polluted soils. Plants not only gather metals but also deposit them as nanoparticles. In summary, reducing agents derived from plants and microbes are used in the biosynthetic process, or biosynthesis, to create nanoparticles (Abass and Alwared, 2024).

The biosynthesis of silver oxide nanoparticles utilizing leaf extract was effectively described in this work. The characteristics of the suggested catalyst were investigated using different assessment techniques, and the removal of black azo dye was examined under visible light exposure considering a variety of reaction parameters.

## MATERIALS AND METHODS

### Materials

The materials utilized in this study included leaves of the Trumpet vine plant, double distilled water that was used as a solvent in various preparation steps, Sodium hydroxide (NaOH), and silver nitrate ($AgNO_3$, 99.8%). The black azo dye, known for its complex molecular structure and environmental persistence, was the specific dye targeted for removal in this study. All chemicals utilized were procured from Thomas Baker, India, and were employed without undergoing any additional purification steps

### Green material preparation

Fresh Trumpet vine leaves were gathered and thoroughly cleaned with double-distilled water. Using a mixer grinder, these leaves were dried and ground into a fine powder. The plant extract was made by dissolving 20 g of powdered leaves in 200 ml of double-distilled water, then boiling

the liquid for 25 minutes at an approximate temperature of 60 °C and stored for further experiments (Haider and Alwared, 2023).

### Green syntheses of silver oxide NPs

Silver ion reduction was used to produce NPs in an environmentally friendly manner. Aqueous solution containing 1 mM silver ions solution (90 ml) was gradually supplemented with 5 ml of leaf extract drop by drop. Initially, the production of silver nanoparticles was verified visually. The reaction turned from a green-dark solution to a goldish-brown color after 5 minutes of constant stirring when the reductant (leaf extract) and silver nitrate were mixed, confirming the synthesis of silver particles (Figure 1). The created NPs were centrifuged for 15 minutes at 10.000 rpm at 40 °C and dried in a hot air oven at 100 °C for 1 hour. Finally, the collected Ag-NPs were stored in a glass bottle for further characterization (Manik et al., 2020).

### Experimental setup

The batch mode reactor used for the tests was made locally out of aluminum. A 12×12×3.8 cm fan running at 2550 rpm ventilates the photoreactor, which creates a closed box of 60×60×60 cm. This ensures that the reactor's air circulates properly. An internal stirrer was positioned in the center of the reactor, with its top surface 13 cm from the bottom. During the trials, the dye solution was kept in a 1000 mL Pyrex glass beaker. For the photocatalytic processes, four 50-watt LED projectors served as the visible light source. To provide even illumination, these projectors were placed around the beaker at 90-degree intervals, with a 10-cm gap between them (Figure 2).

## RESULTS AND DISCUSSION

Trumpet vine extract was used to successfully synthesize $Ag_2O$ nanoparticles (NPs) as capping and reducing agents. By examining their optical, morphological, and biological characteristics, silver nanoparticles were investigated. Utilizing an X-ray diffractometer, Fourier transform-infrared spectroscopy, UV-visible spectroscopy, and scanning electron microscopy with the elemental dispersive spectrum, photoluminescence, photocatalytic activity, and photoluminescence, silver oxide nanoparticles were characterized.


**Figure 1.** Flowchart illustrates the green synthesis process of $Ag_2O$ nanoparticles

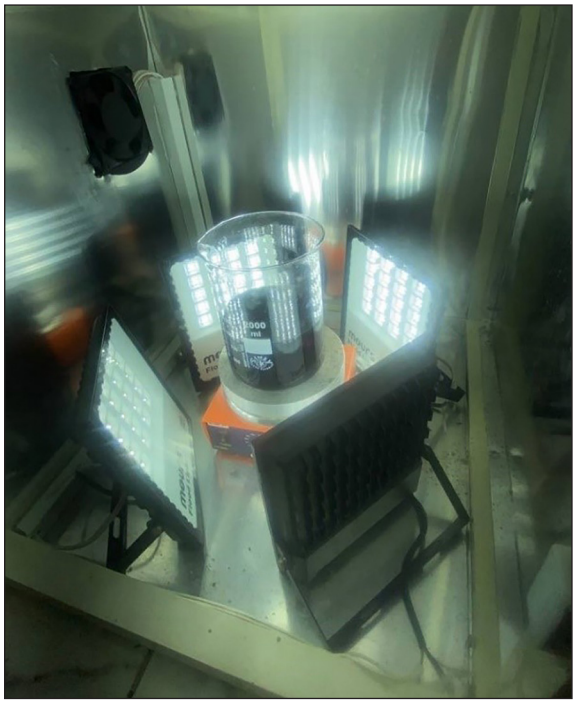

**Figure 2.** Batch configuration with LED projectors used for the photocatalytic reaction

## Characterization of $Ag_2O$ NPs

### *Elemental composition*

An energy-dispersive X-ray spectroscope (EDS) fitted with a SEM was also used to analyze the chemical composition of the silver particles. A prominent silver signal in the EDS profile indicated that silver (Ag) was a significant component of the produced particles. According to the EDS spectra, the synthesized samples are dominant silver (shown by distinct Ag peaks) with minor peaks of oxygen (O), carbon (C), and iron (Fe (as illustrated in Figure 3. These secondary components are attributed to the organic ingredient of trumpet vine extract that is used as a capping and stabilizing agent (Al-Musawi et al., 2023; Kadam et al., 2016).

### *Morphology analysis*

The synthesized $Ag_2O$ NPs' morphology was investigated using scanning electron microscopy (SEM) examination. The uncapped silver nanoparticles showed agglomerated uneven shapes as can be seen in (Figure 4A). By using the leaf extract as a modifier, the nanoparticles, which had a minimum size of 31.82 nm, showed a plate-like shape with sharp numerous facets indicating that Particle size is determined by the proportion of stabilizing agent to silver ions (Figure 4B). Therefore, the creation of Ag2O NPs may have been influenced by a variety of parameters, such as time and the concentration of the reducing agents. Aside from that, stabilizing agents are important because they prevent the particles from clumping together, which helps manage their form (Ali and Alwared, 2024a; Mohammed et al., 2024).

### *Structural characterization*

The structural analysis of the nanoparticles was assessed through an X-ray diffraction (XRD)

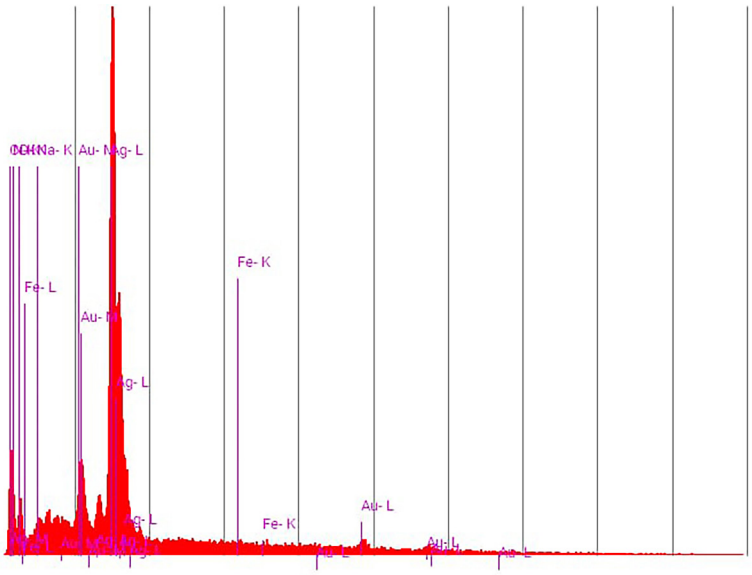


**Figure 3.** Element analysis profile of the synthesized $Ag_2O$ nanoparticles using dispersive X-ray spectroscope (EDS)

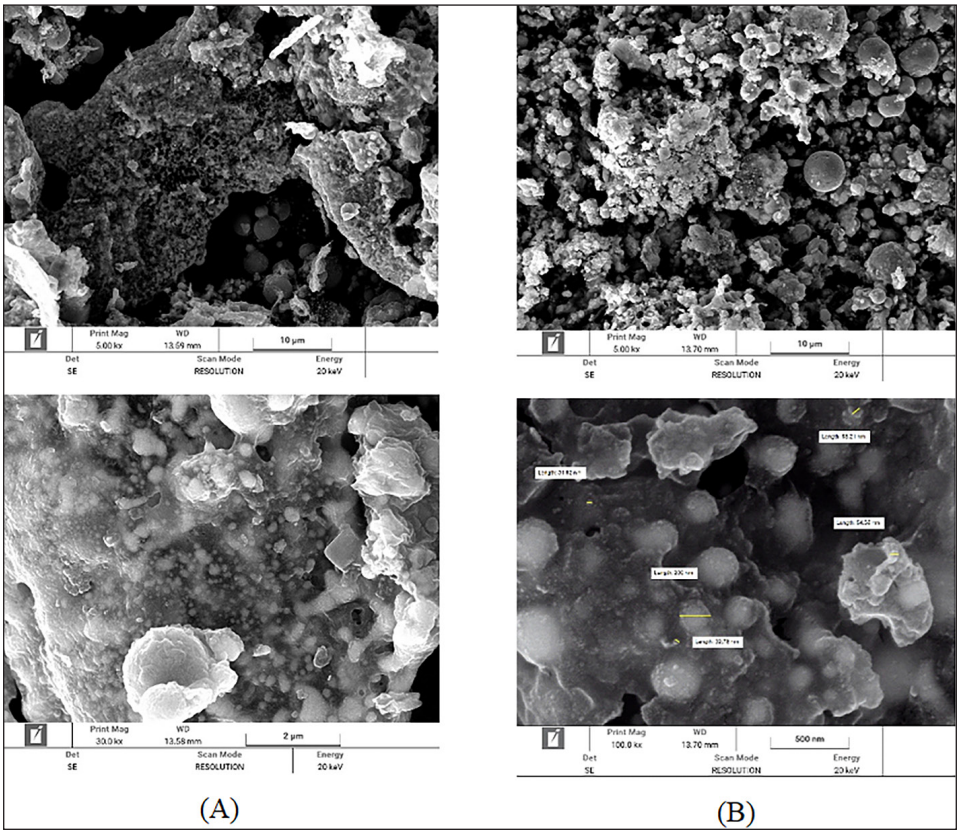


**Figure 4.** Images of various magnification factors showing the morphology of $Ag_2O$ nanoparticles using scanning electron microscopy (SEM)

test. The results presented in (Figure 5) reveal multiple distinctive peaks that likely correspond to the typical face-centered cubic (FCC) structure of silver. The observed positions of peaks were at 38.3°, 44.5°, 64.6°, and 77.5° which corresponded to 111, 200, 220, and 311 planes respectively. The slight broadening of these peaks suggests a nanoscale size of the specimen and the high-intensity reflection of the 111 plane indicates that the silver NPs have preferred orientation along this plane. Additionally, the crystal size was further quantified for the 111-reflection plane using the Scherrer equation and was found to be 7.4 nm. Overall, the results suggest that the silver nanoparticles are relatively pure and free from secondary phases (Kazlagić et al., 2020).

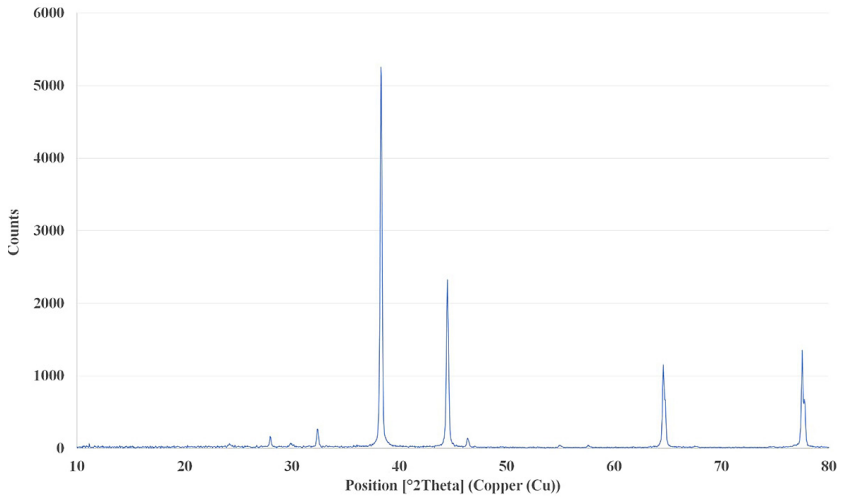


**Figure 5.** XRD results for the $Ag_2O$ nanoparticles

*Surface properties of silver NPs*

The surface area of the nanomaterial was calculated through the Brunauer-Emmett-Teller (BET) and Langmuir Isotherm illustrated in (Figure 6A) and (Figure 6B), respectively. The total specific area revealed by the BET test is 16.361 $m^2$ $g^{-1}$, however, if a homogenous surface assumption was utilized, then the maximum adsorption area produced by Langmuir Isotherm is 28.263 $m^2$ $g^{-1}$. The surface area of nanoscale particles is usually categorized under two distinctive regions, the Micropore and the Mesopore. The Micropore is for particles with small sizes of less than 2 nm while the Mesopore zone involves particles size between (2–50 nm). The t-plot presented in (Figure 6C) is

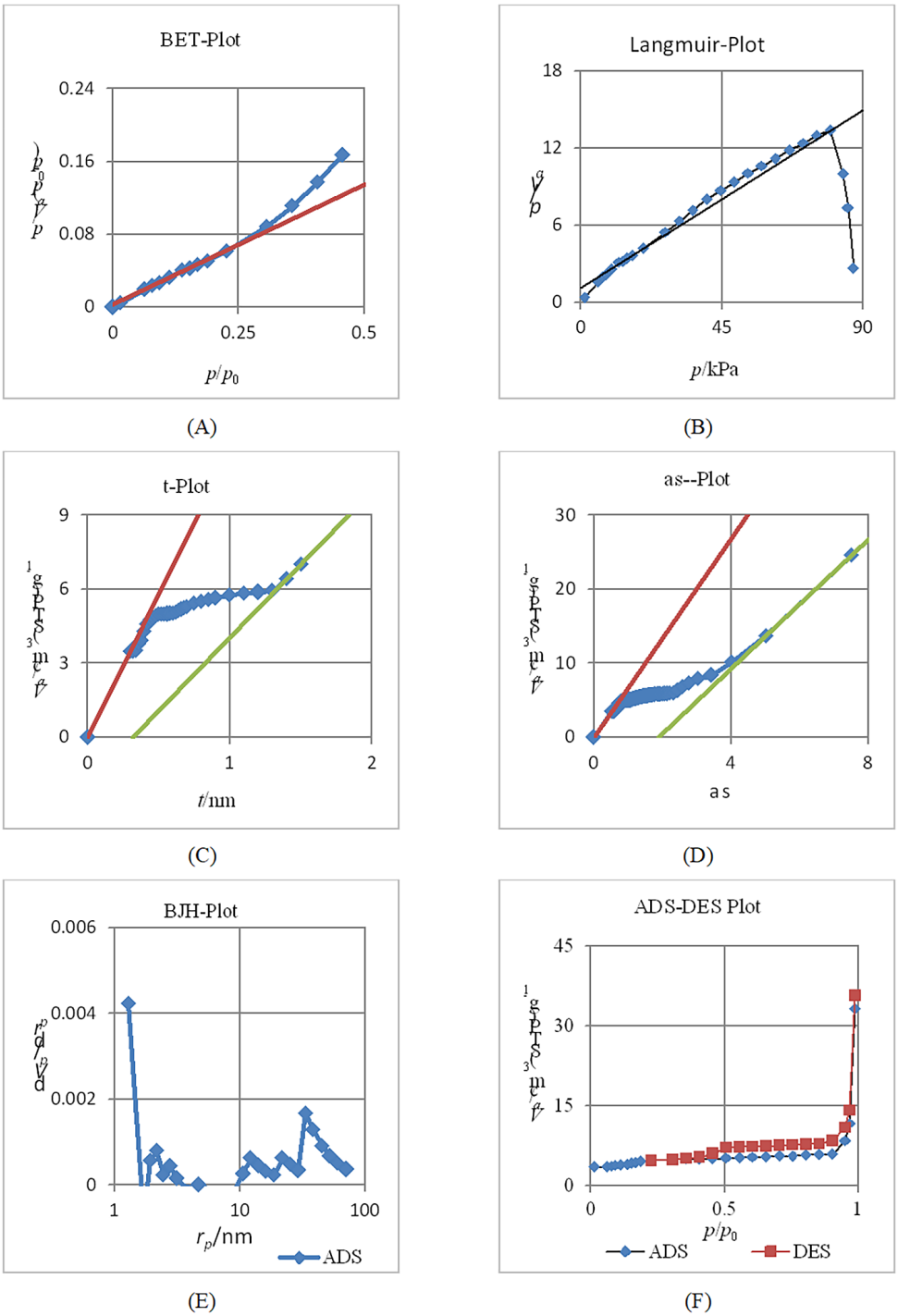


**Figure 6.** BET Surface area and porosity analysis of the $Ag_2O$ nanoparticles, (A) BET, (B) Langmuir, (C) t-plot, (D) αs- plot, (E) BJH, (F) ADS-DES

used to differentiate these two areas. Accordingly, a greater area contribution is found to be yielded from the Mesopore zone with 17.835 $m^2 g^{-1}$ compared to only 9.097 $m^2 g^{-1}$ participated by the Micropore, indicating the high efficiency of the trumpet vine leaf extract as a reducing and capping agent. Further inspection was done using αs-plot (Figure 6D) and a comparable result was found confirming the t-plot outcomes (Mesoporosity = 18.154 $m^2 g^{-1}$, Microporosity = 11.865 $m^2 g^{-1}$). Additionally, the Barrett-JoynerHalenda (BJH) method was used to examine the Mesoporosity pore size distribution of the sample resulting in a 6.939 $m^2 g^{-1}$ pore area (Figure 6E). The Overall Adsorption-Desorption behavior is demonstrated in (Figure 6F). The isotherm shows a sharp increase in adsorption volume compatible with Type IV isotherms. This is commonly associated with mesoporous materials further emphasizing the results of t-plot and αs-plot (Alwared et al., 2023b; Wang et al., 2020).

### *Fourier transform infrared spectroscopy (FTIR) analysis*

The surface functional groups and their interactions found in the synthesized Ag-NPs were identified using FTIR analysis. (Figure 7) displays the as-prepared Ag-NPs' pragmatic FTIR spectrum. The extract's phytochemicals functioned as a capping agent, binding to the Ag-NPs, as evidenced by the major absorption peaks of 3420.14 (O-H, stretch, H-bonded), 1600.63, 1457.92, 1254.47, 1096.33, 873.596, and 615.181 $cm^{-1}$. These can be attributed to O–H, C–C, C–H band, –C–O, –C–H (alkanes), and COO– stretching vibrations, respectively (Ali et al., 2023). The presence of phytochemicals in the Trumpet vine extract, such as amide groups, amino groups, carboxyl groups, tannins, phenol, flavonoids, terpenoids, saponins, and polyphenolic compounds, was found to be crucial for the reduction, capping, and stabilization of Ag-NPs, as determined by FTIR analysis.

## Photocatalytic activity

### *Dye removal*

The removal efficiency of black azo dye was investigated under various concentrations of the catalyst (green-enhanced silver nanoparticles). Figure 8A illustrates the role of catalyst dosage on the degradation rates of the pollutant (Azo dye). Five catalyst concentrations were examined (0.2 g/L, 0.4 g/L, 0.6 g/L, 0.8 g/L, 1.0 g/L) after optimizing the concentration of the black dye and pH value at 15 mg/L and 5, respectively. A pH of 5.0 was selected for the experiment as it represents a typical slightly acidic environment, which closely mimics real-world conditions for pollutant degradation and is known to enhance photocatalytic activity by promoting the generation of reactive oxygen species (ROS) without causing excessive catalyst instability (Haider and Alwared, 2023). There are two stages for conducting the test, the first stage is the adsorption phase which is performed in the dark state, and the second stage is the photocatalytic phase which is performed under visible light irradiation. The adsorption period took place in 30 minutes and negligible removal rates were noticed (Aravind et al., 2021). However, under visible light conditions, the degradation efficiency rapidly increases with time reaching a maximum removal efficiency of 79% using 1.0 g/L catalyst (Equation 1). Decreasing dosages of the silver nanoparticles

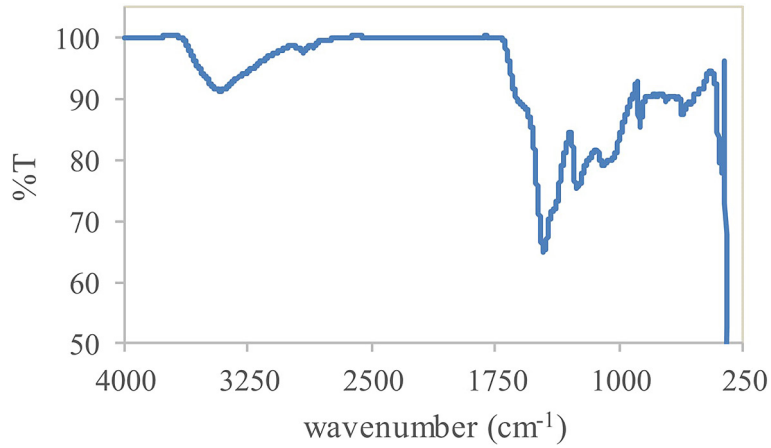


**Figure 7.** FTIR spectra of $Ag_2O$ NPS

revealed lower degradation rates with an average effectiveness of 75%. Additionally, a kinetic analysis was performed in order to specify the reaction type. Two reaction models were investigated, the first-order and second-order kinetic models illustrated in Equation 2 and Equation 3, respectively (Abdulrazaq et al., 2023; Mohammed et al., 2020).

$$Removal\ Efficiency = 100 \times \left(1 - \frac{C}{C_0}\right) \quad (1)$$

$$Ln\left(\frac{C}{C_0}\right) = -k_1 t \quad (2)$$

$$\left(\frac{1}{C}\right) - \left(\frac{1}{C_0}\right) = k_2 t \quad (3)$$

where: $C_o$ is the initial concentration of the pollutant, $C$ is the pollutant concentration under light irradiation for a specific time ($t$), and $k_1$ and $k_2$ are the kinetic rate constants for first and second kinetic models (Ali and Alwared, 2024b; Raghad and Abeer, 2023).

Figure 8B and Figure 8C demonstrate the profiles of the suggested models for a variety of catalyst concentrations with time. The straight line of the first-order model aligns perfectly with the data points, suggesting an excellent representation of the reaction. On the other hand, the second-order model differs considerably and there is a poor matching between the points and the straight line. These results

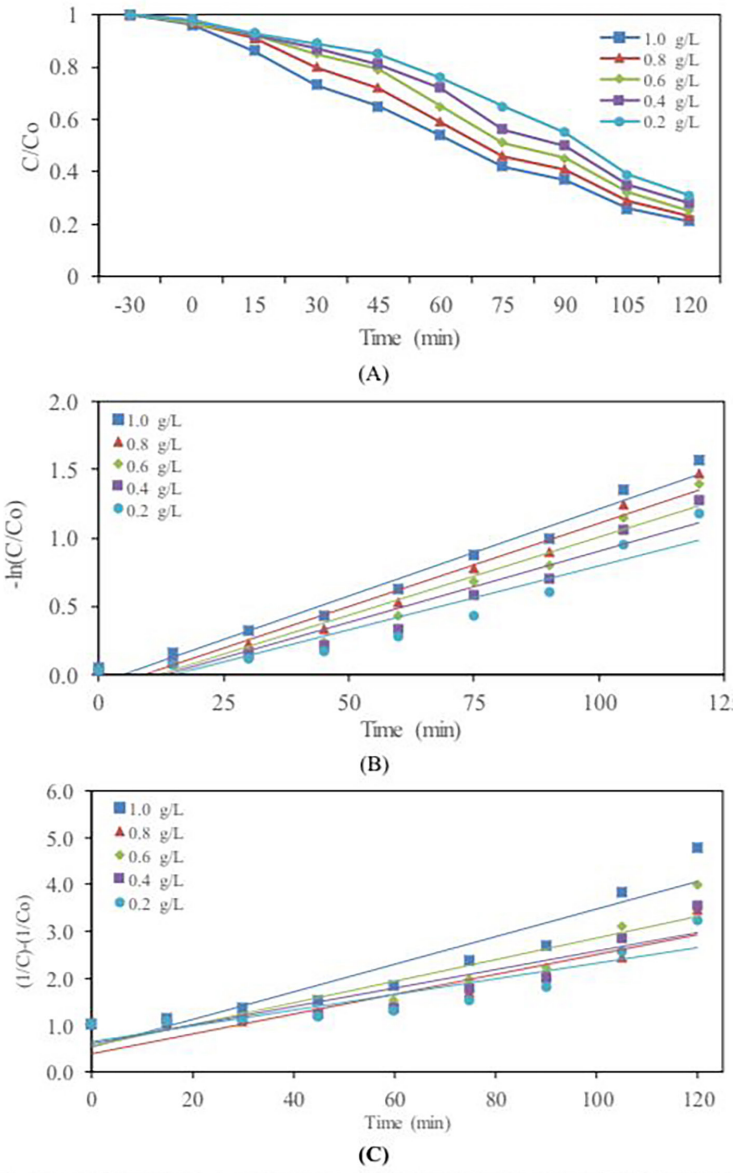


**Figure 8.** Dye removal efficiency under visible light: (A) Degradation rate of Azo dye (B) first order kinetic model, (C) second order kinetic model

**Table 1.** Kinetic model study using various catalyst concentrations

| Catalyst dosage (g/L) | 1st Order | | 2nd Order | |
|---|---|---|---|---|
| | $K_1$ ($min^{-1}$) | $R^2$ | $K_2$ (L/mol/min) | $R^2$ |
| 1.0 | 0.0127 | 0.9787 | 0.0294 | 0.8865 |
| 0.8 | 0.0122 | 0.9662 | 0.0231 | 0.8484 |
| 0.6 | 0.0114 | 0.9434 | 0.0212 | 0.8788 |
| 0.4 | 0.0104 | 0.9244 | 0.0197 | 0.8321 |
| 0.2 | 0.0094 | 0.8943 | 0.0167 | 0.8022 |

are numerically presented in Table 1. The correlation coefficients ($R^2$) of the first-order model are significantly higher for the whole series compared to the second-order type, further confirming the reliability of the first-order kinetic to describe the reaction process. Hence, the photocatalytic reaction was suggested to follow the pseudo-1st-order kinetic model with a highest value of reaction constant ($K_1$) of 0.0127 $min^{-1}$ at 1.0 g/L concentration and a correlation coefficient $R^2 = 0.9787$.

### *Repeatability analysis*

In order to confirm the reliability of the proposed photocatalyst, a stability study consisting of five cycles was performed by collecting the silver NPs after each cycle and using them again for the dye removal reaction. An optimum parametric value of 1.0 g/L photocatalyst dosage, 15 mg/L dye concentration, and pH of 5 were utilized for that purpose. As can be demonstrated in (Figure 9), the catalyst is approved to be stable and can be reused for several runs while retaining its effectiveness. The maximum reduction in the degradation efficiency was 12.6% after five consecutive runs, affirming the stability of the bio-improved silver nanoparticles for the treatment of black azo dye.

### *Comparison with previous studies*

The photodegradation performance of this study was compared with other previous research to evaluate the photodegradation activity of $Ag_2O$ NPs, and the results are presented in Table 2. The targeted pollutant for all of the selected studies was a variety of black azo dye treated by silver nanoparticles that were synthesized using different green pathways. Several variables were taken into account, including direct parameters like the concentration of pollutants, the dose of catalyst, the duration of irradiation, and the removal efficiency. Undirect parameters such as cost, environment, and feasibility were also considered to conclude a holistic assessment for the comparison.

It was noticed that some of these studies have taken a long time to prepare the $Ag_2O$ NPs for up to 168 h of mixing were utilized to formulate the nanomaterial (Kumar et al., 2016) compared to less than 2 h needed for this study. Other studies demand 8 h to reach the maximum removal efficiency under sunlight (Kumar et al., 2016; Roy et al., 2015) which represents a whole sunny day in an optimistic estimation compared to only two hours of LED light exposure suggested by this

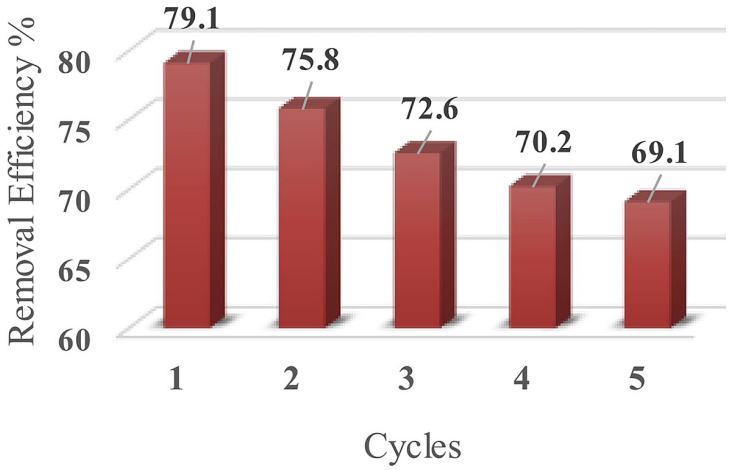


**Figure 9.** Stability analysis of the bio-enhanced silver nanoparticles

**Table 2.** Previous studies on the green synthesis of $Ag_2O$ NPs and its efficiency in removing pollutants

| Plant name | Catalyst dose | Pollutant dose | Light source | Time (h) | Efficiency (%) | References |
|---|---|---|---|---|---|---|
| Potato (*Solanum tuberosum*) | 500 mg/L | 10 mg/L | Sunlight | 8 | 75 | (Roy et al., 2015) |
| *Lantana camara* L. flower | 0.2–1.0 mL | 10 mg/L | Sunlight | 6 | 70.6 | (Kumar et al., 2016) |
| *Bacillus licheniformis* | 200 mg/L | 10 mg/L | Visible light | 3 | 94.0 | (Momin et al., 2019) |
| *Nepeta leucophylla* | 1.8 ml | 60 mg/L | Mercury Lamp 125 Watts | 3 | 82.8 | (Singh & Dhaliwal, 2020) |
| Jasmine flower extract | 10 mg | 100 ml | Sunlight | 2 | 72.0 | (Aravind et al., 2021) |
| Trumpet vine leaves | 0.2–1.0 g/L | 15 mg/L | Visible light | 2 | 79.1 | This study |

work. Additionally, the highest degradation efficiency of all these studies was 94% (Momin et al., 2019). This percentage was achieved using mutant Bacillus licheniformis as a bio ingredient which is a genetically modified mutation of the Bacillus bacteria that can developed by special medical laboratories in sample form with high production cost and these samples are not adequate for real-life scenarios where high discharge wastewater are expected. There are also region-specific plants that are habited to certain areas like the Nepeta leucophylla, a plant found in extremely high elevations mainly in the Himalayas (Singh and Dhaliwal, 2020). Other studies have used the flowers of plants instead of their leaves for instance the Jasmine flower (Aravind et al., 2021), and Lantana camara flower (Kumar et al., 2016). This part of the plant is usually seasonal and has other medical and commercial uses making it costly with limited availability. This work has used the leaves of the trumpet vine plant, known for its aggressive overgrowth, worldwide climate adaptation, and partly evergreen (The U.S. Department of Agriculture (USDA)).

## CONCLUSIONS

The improved silver nanoparticles with the green-like material of the Trumpet vine leaf extract have approved its effectiveness as a photocatalyst in the removal of black azo dye from an aqueous solution, removal efficiency was 79.1% after 2 hours of visible light exposure using 1.0 g/L of catalyst dosage, 15 mg/L of dye concentration, and pH value of 5. The characterizations of the $Ag_2O$ NPs were identified using XRD, FTIR, SEM, and BET techniques. The role of the green material as a capping agent was specifically revealed in the characterization analysis of the proposed nanomaterial. The adaption of visible light irradiation with leaf extract in the ignition of the reaction activity is a convenient, environmentally friendly for water treatment. Additionally, the reusability study and kinetic analysis further emphasize its reliability in maintaining the degradation rates. These results introduce a strong catalyst for multiple applications where the environment is a key factor in the treatment process.

## REFERENCES

1. Abass, I. S., & Alwared, A. I. (2024). Bio-synthesis and photocatalytic activity of zinc oxide nanoparticles for sulfosulfuron herbicide degradation from aqueous solutions. *Journal of Ecological Engineering, 25*(12), 181–193. https://doi.org/10.12911/22998993/194177
2. Abdulrazaq, H. A., Alwared, A. I., & Onyeaka, H. (2023). Ibuprofen degradation from synthetic wastewater using photo-Fenton process. *Iraqi Journal of Chemical and Petroleum Engineering, 24*(4), 107–114. https://doi.org/10.31699/ijcpe.2023.4.11
3. Akhtar, M. S., Panwar, J., & Yun, Y. S. (2013). Biogenic synthesis of metallic nanoparticles by plant extracts. *ACS Sustainable Chemistry and Engineering, 1*(6), 591–602. https://doi.org/10.1021/sc300118u
4. Al-Musawi, T. J., Mengelizadeh, N., Alwared, A. I., Balarak, D., & Sabaghi, R. (2023). Photocatalytic degradation of ciprofloxacin by MMT/$CuFe_2O_4$ nanocomposite: characteristics, response surface methodology, and toxicity analyses. *Environmental Science and Pollution Research, 30*(27), 70076–70093. https://doi.org/10.1007/s11356-023-27277-7
5. Ali, A. H., & Alwared, A. I. (2024a). Construction of ternary heterostructure of zeolite/$Fe_3O_4$/CuS/$CuWO_4$ as a reusable: Characterization studies.

Asia-Pacific *Journal of Chemical Engineering, 19*(5), e3125. https://doi.org/10.1002/apj.3125

6. Ali, A. H., & Alwared, A. I. (2024b). Photocatalytic continuous degradation of pharmaceutical pollutants by zeolite/$Fe_3O_4$/CuS/$CuWO_4$ nanocomposite under direct sunlight. *Results in Engineering, 24*, 103234. https://doi.org/10.1016/j.rineng.2024.103234
7. Ali, Q. A., Shaban, M. A. A., Mohammed, S. J., M-Ridha, M. J., Abd-Almohi, H. H., Abed, K. M., Salleh, M. Z. M., & Hasan, H. A. (2023). Date palm fibre waste exploitation for the adsorption of congo red dye via batch and continuous modes. *Journal of Ecological Engineering, 24*(10), 259–276. https://doi.org/10.12911/22998993/169176.
8. Alwared A. I., Mohammed N. A., Al-Musawi T. J. and Mohammed A. A. (2023a), Solar-induced photocatalytic degradation of reactive red and turquoise dyes using a titanium oxide/xanthan gum composite, *Sustainability, 15*(14), 10815; https://doi.org/10.3390/su151410815
9. Alwared, A. I., Sulaiman, F. A., Raad, H., Al-Musawi, T. J., & Mohammed, N. A. (2023b). Ability of $FeNi_3$/$SiO_2$/$TiO_2$ nanocomposite to degrade amoxicillin in wastewater samples in solar light-driven processes. *South African Journal of Botany, 153*, 195–202. https://doi.org/10.1016/j.sajb.2022.12.031
10. Aravind, M., Ahmad, A., Ahmad, I., Amalanathan, M., Naseem, K., Mary, S. M. M., Parvathiraja, C., Hussain, S., Algarni, T. S., Pervaiz, M., & Zuber, M. (2021). Critical green routing synthesis of silver NPs using jasmine flower extract for biological activities and photocatalytical degradation of methylene blue. *Journal of Environmental Chemical Engineering, 9*(1), 104877. https://doi.org/10.1016/j.jece.2020.104877
11. Donkadokula, N. Y., Kola, A. K., Naz, I., & Saroj, D. (2020). A review on advanced physico-chemical and biological textile dye wastewater treatment techniques. *Reviews in Environmental Science and Biotechnology, 19*(3), 543–560. https://doi.org/10.1007/s11157-020-09543-z
12. Feng, P., Zhou, Q. L., Guan, X. H., & Zhou, G. M. (2014). Preliminary study on the effect of zero valent iron enhanced by weak magnetic field on the AZO dyes decoloration in the water. *Sichuan Environ, 33*(4), 1–6.
13. Haider, F. A., & Alwared, A. I. (2023). Solar photocatalytic degradation of metronidazole antibiotic by bio-synthesis Tio2 from aqueous solution: Effect of solar intensity and Ph. *Ann. For. Res, 66*(1), 4081–4093. www.e-afr.org
14. Hemlata, Meena, P. R., Singh, A. P., & Tejavath, K. K. (2020). Biosynthesis of silver nanoparticles using cucumis prophetarum aqueous leaf extract and their antibacterial and antiproliferative activity against cancer cell lines. *ACS Omega, 5*(10), 5520–5528. https://doi.org/10.1021/acsomega.0c00155
15. Kadam, A., Dhabbe, R., Gophane, A., Sathe, T., & Garadkar, K. (2016). Template free synthesis of ZnO/$Ag_2O$ nanocomposites as a highly efficient visible active photocatalyst for detoxification of methyl orange. *Journal of Photochemistry and Photobiology B: Biology, 154*, 24–33. https://doi.org/10.1016/j.jphotobiol.2015.11.007
16. Kazlagić, A., Abud, O. A., Ćibo, M., Hamidović, S., Borovac, B., & Omanović-Mikličanin, E. (2020). Green synthesis of silver nanoparticles using apple extract and its antimicrobial properties. *Health and Technology, 10*(1), 147–150. https://doi.org/10.1007/s12553-019-00378-5
17. Kumar, B., Smita, K., & Cumbal, L. (2016). Biosynthesis of silver nanoparticles using Lantana camara flower extract and its application. *Journal of Sol-Gel Science and Technology, 78*(2), 285–292. https://doi.org/10.1007/s10971-015-3941-8
18. Manik, U. P., Nande, A., Raut, S., & Dhoble, S. J. (2020). Green synthesis of silver nanoparticles using plant leaf extraction of Artocarpus heterophylus and Azadirachta indica. *Results in Materials, 6*, 100086. https://doi.org/10.1016/j.rinma.2020.100086
19. Mohammed, N. A. A., I. Alwared, A., & S. Salman, M. (2020). Decolorization of Reactive Yellow Dye by Advanced Oxidation Using Continuous Reactors. *Iraqi Journal of Chemical and Petroleum Engineering, 21*(2), 1–6. https://doi.org/10.31699/ijcpe.2020.2.1
20. Mohammed, N. A., Alwared, A. I., Shakhir, K. S., & Sulaiman, F. A. (2024). Synthesis, characterization of FeNi3@SiO2@CuS for enhance solar photocatalytic degradation of atrazine herbicides: Application of RSM. *Results in Surfaces and Interfaces, 16*, 100253. https://doi.org/10.1016/j.rsurfi.2024.100253
21. Momin, B., Rahman, S., Jha, N., & Annapure, U. S. (2019). Valorization of mutant Bacillus licheniformis M09 supernatant for green synthesis of silver nanoparticles: photocatalytic dye degradation, antibacterial activity, and cytotoxicity. *Bioprocess and Biosystems Engineering, 42*(4), 541–553. https://doi.org/10.1007/s00449-018-2057-2
22. Okab, A A, and Alwared A I, 2023. A dual S-scheme g-C3N4/Fe3O4/Bi2WO6/Bi2S3 heterojunction for improved photocatalytic decomposition of methylene blue: Proposed mechanism, and stability studies, *Materials Science in Semiconductor Processing, 153*, (2023), 107196.
23. Raghad, N. M., & Abeer, I. A. (2023). Adsorption of methylene blue from aqueous solution using free and immobilized Algae Cells. *Iraqi Journal of Agricultural Sciences, 54*(5), 1387–1397. https://doi.org/10.36103/ijas.v54i5.1839

24. Rasouli J, Binazadeh M, and Sabbaghi S. (2024). Synthesis of a novel biomass waste- based photocatalyst for degradation of high concentration organic pollutants under visible light: Optimization of synthesis condition and operational parameters via RSM-CCD, *Surfaces and Interfaces, 49*, 104400.
25. Roy, K., Sarkar, C. K., & Ghosh, C. K. (2015). Photocatalytic activity of biogenic silver nanoparticles synthesized using potato (Solanum tuberosum) infusion. Spectrochimica Acta Part A: *Molecular and Biomolecular Spectroscopy, 146*, 286–291.
26. Sarkar, S., Banerjee, A., Chakraborty, N., Soren, K., Chakraborty, P., & Bandopadhyay, R. (2020). Structural-functional analyses of textile dye degrading azoreductase, laccase and peroxidase: A comparative in silico study. *Electronic Journal of Biotechnology, 43*, 48–54. https://doi.org/10.1016/j.ejbt.2019.12.004
27. Singh, J., & Dhaliwal, A. S. (2020). Plasmon-induced photocatalytic degradation of methylene blue dye using biosynthesized silver nanoparticles as photocatalyst. *Environmental Technology (United Kingdom), 41*(12), 1520–1534. https://doi.org/10.1080/09593330.2018.1540663
28. Singh, R. L., Singh, P. K., & Singh, R. P. (2015). Enzymatic decolorization and degradation of azo dyes - A review. *International Biodeterioration and Biodegradation, 104*, 21–31. https://doi.org/10.1016/j.ibiod.2015.04.027
29. Sinha, A., Lulu, S., Vino, S., Banerjee, S., Acharjee, S., & Jabez Osborne, W. (2018). Degradation of reactive green dye and textile effluent by Candida sp. VITJASS isolated from wetland paddy rhizosphere soil. *Journal of Environmental Chemical Engineering, 6*(4), 5150–5159. https://doi.org/10.1016/j.jece.2018.08.004
30. Wang, Y., Bi, N., Zhang, H., Tian, W., Zhang, T., Wu, P., & Jiang, W. (2020). Visible-light-driven photocatalysis-assisted adsorption of azo dyes using Ag2O. In Colloids and Surfaces A: Physicochemical and Engineering Aspects. *Physicochemical and Engineering Aspects, 585*, p. https://doi.org/10.1016/j.colsurfa.2019.124105
31. Yong, X., & Schoonen, M. A. A. (2000). The absolute energy positions of conduction and valence bands of selected semiconducting minerals. *American Mineralogist, 85*(3–4), 543–556. https://doi.org/10.2138/am-2000-0416
32. Zhu, C., Guo, S., Fang, Y., & Dong, S. (2010). Reducing sugar: New functional molecules for the green synthesis of graphene nanosheets. *ACS Nano, 4*(4), 2429–2437. https://doi.org/10.1021/nn1002387
33. Narayanan, K.B. and Sakthivel, N. (2010). Biological synthesis of metal nanoparticles by microbes. Advances in colloid and interface science, 156(1–2): 1–13.
34. Jalill, A., Raghad, D.H., Nuaman, R.S. and Abd, A.N. (2016). Biological synthesis of Titanium Dioxide nanoparticles by Curcuma longa plant extract and study its biological properties. World Scientific News, 49(2): 204–222.
35. Parveene, K., Banse, V. and Ledwani, L. (2016), April. Green synthesis of nanoparticles: their advantages and disadvantages. In *AIP conference proceedings 1724*(1), 020048. AIP Publishing LLC.